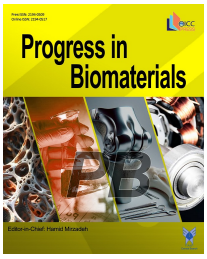

Volume 12, Issue 4, 122319 (1-14)

Progress in Biomaterials (PIBM)

https://doi.org/10.57647/pibm.2023.122319

Evaluation of the Performance of a Targeted Dermal Drug Delivery System: Magnetic Liposome/$CoFe_2O_4$/Ascorbic Acid Nanocarrier

Mojdeh Khosravi Farahani[1], Parviz Aberoomand Azar[1], Mohammad Yousefi[2,*], Maryam Bikhof Torbati[3]

[1]*Department of Chemistry, SR.C., Islamic Azad University, Tehran, Iran.*
[2]*Department of Chemistry, TeMS.C., Islamic Azad University, Tehran, Iran.*
[3]*Department of biology, YI.C., Islamic. Azad University, Tehran, Iran.*

[*]**Corresponding author:** myousefi50@iau.ac.ir

Original Research

Received:
10 August 2023
Revised:
18 October 2023
Accepted:
22 October 2023
Published online:
30 December 2023

Abstract:

The transdermal drug delivery system represents a non-invasive and proficient approach that facilitates gradual release of pharmaceuticals while targeting the specific site of action. This modality has the potential to enhance both the therapeutic effectiveness and safety profiles of medications, sustain consistent plasma concentrations of the drug, circumvent first-pass hepatic metabolism, and offers a method that is both convenient and devoid of pain. The use of nanocarriers such as magnetic liposome/$CoFe_2O_4$ is known for targeted drug delivery. In this study, magnetic liposome/$CoFe_2O_4$ nanocarrier was synthesized and characterized. Then, ascorbic acid with high antioxidant properties was encapsulated in magnetic liposome/$CoFe_2O_4$ nanocarrier. In the next step, the absorption of ascorbic acid was evaluated by various parameters such as ascorbic acid concentration (mg/L), pH, time (min), and weight percentage of $CoFe_2O_4$ (wt%) by experimental design and Box-Behnken method. Under optimal conditions, the highest absorption rate was obtained with a concentration of ascorbic acid 11.99 mg/L, a time of 27.43 minutes, pH = 8.78 and a weight percentage of 13.85% $CoFe_2O_4$, equal to 99.99%. The nanoliposome/$CoFe_2O_4$/ascorbic acid formulation achieved controlled release, with $< 20\%$ released in the first hour and 86% by 12 hours. Ex-vivo studies showed $\sim 65\%$ steady permeation compared to $< 60\%$ burst permeation for free ascorbic acid in 8 hours, highlighting superior controlled delivery.

Keywords: Nanocarrier; magnetic liposome/$CoFe_2O_4$; Ascorbic acid; Optimization; Release

Cite this article: Khosravi Farahani, M., Aberoomand Azar, P., Yousefi, M., Bikhof Torbati, M. Evaluation of the Performance of a Targeted Dermal Drug Delivery System: Magnetic Liposome/$CoFe_2O_4$/Ascorbic Acid Nanocarrier. *Progress in Biomaterials* **12**(4), Article 19 (2023).

1. Introduction

Despite the great amount of research that has been done in the field of skin and dermal drug delivery, finding an effective method for local drug delivery to the skin is still a challenge (Alkilani et al., 2022). In response to the need for effective drug delivery to the skin, Touitou first designed a phospholipid vesicular nanocarrier called ethosome in 1996 (Gupta and Trivedi, 2018). This vesicular carrier is distinguished from other lipid carriers by some important features, including vesicle bilayer fluidity, enhanced penetration mechanism, simple preparation, and lack of side effects. Ethosomes have been well studied for various dermal drug delivery applications since their introduction. Transdermal permeability refers to the delivery of drugs into the body through the skin for local or systemic treatment. Trans dermally adsorbed drugs are free from hepatic first-pass effects and gastrointestinal side effects (Akbari et al., 2022). The use of chemical absorption enhancers and physical absorption enhancer systems is less used today, in addition to being expensive and causing changes on the skin, and the future is looking to the use of new technologies. One of the most important new technologies in the field of transdermal drug delivery is the use of pharmaceutical nanocarriers (De Oliveira et al., 2022; Jeong et al., 2021). Smaller particles

are more easily adsorbed and penetrated through the skin surface. Transdermal nano formulations, as systems that increase drug absorption, increase formulation stability, and deliver drugs to the target, are widely used in pharmaceuticals today (Alkilani et al., 2022).

Phospholipids, with or without cholesterol, are the primary constituents of liposomes. Typically, phospholipid molecules consist of two distinct polarities: Hydrophilic and lipophilic. Hydrocarbon chains of different lengths act as lipophilic poles. Liposomes are formed spontaneously after vesicle formation in aqueous solution (Xiao et al., 2022). The unique structure of liposomes has led to the formulation of both hydrophilic and lipophilic molecules with these carriers. Recent studies show that antioxidants are important nutritional factors and play an important role in the functioning of the human immune system (Ahmed et al., 2019). Therefore, it is necessary to use strategies to control the release and maintenance of antioxidants in the cells and tissues of the human body. Today, targeted and sustained release of products in the human body has become possible through encapsulation methods. Also, nanotechnology has had more impact on many aspects of people's lives than any other scientific discovery, and it can be said that the targeted release of any compound in the body is affected by the size of the nanoparticles. Encapsulating these antioxidant compounds within multilayer vesicles and phospholipids increases the absorption and penetration of these nanoparticles (Sun et al., 2023). Therefore, nanoencapsulation methods of antioxidants have the ability to increase intracellular penetration and diffusion, increase absorption, protect the compound from degradation, and increase the shelf life and storage of these substances in the human body (Pisoschi et al., 2018; Queiroz et al., 2022).

Ascorbic acid (vitamin C) has wide applications in medicine and skin care due to its antioxidant properties, stimulation of collagen synthesis, and skin lightening. However, its instability to environmental factors such as light, oxygen, and temperature poses a major challenge in its effective use. The rapid degradation of vitamin C into inactive compounds such as dehydroascorbic acid reduces its effectiveness (Yin et al., 2022). To solve this problem, various methods have been investigated, such as the use of more stable derivatives or protected formulations. In the meantime, liposomal nanocarrier technology has been proposed as a promising solution. Liposomes, as biocompatible and biodegradable nanocarriers, can encapsulate ascorbic acid in their lipid bilayer structure and prevent its degradation (Wang et al., 2023). This system not only increases the stability of vitamin C against damaging factors, but also improves its skin permeability and absorption. Studies have shown that liposomal formulations of ascorbic acid have higher bioavailability, lower toxicity, and longer efficacy than its free forms. Therefore, this technology could create a significant revolution in the production of pharmaceutical and cosmetic-health products containing vitamin C (Baek et al., 2021).

Magnetic nanoparticles represent a significant and extensively utilized category of nanomaterials, whose distinctive characteristics endow them with specialized functionalities that distinguish them from other nanostructures (Abdolmohammadi et al., 2020; Vandani et al., 2023). $CoFe_2O_4$ nanoparticles are an ideal choice for dermal applications compared to other magnetic nanoparticles such as Fe_3O_4 due to their superior magnetic properties, high chemical stability, and favorable biocompatibility. These nanoparticles, with their stronger magnetic moment and oxidation resistance, allow for more precise control of drug delivery and imaging. The novelty of using $CoFe_2O_4$ in dermal applications stems from its ability to more precisely target skin tissues and reduce side effects compared to traditional nanoparticles, making it an innovative candidate for advanced dermal therapies (Elmi Fard and Fazaeli, 2022). Magnetization of nanoliposomes in drug delivery has significant advantages, including increased precision targeting of diseased tissues by guiding an external magnetic field, which reduces side effects and increases drug efficacy. This method allows for controlled drug release, especially in the treatment of cancers and inflammatory diseases that require delivering the optimal dose to the exact site of damage. Magnetic nanoliposomes are also more stable in the bloodstream and can be used as diagnostic agents in medical imaging.

Experimental design is the process of systematically planning and organizing a scientific study that aims to test hypotheses or answer research questions (Fard and Fazaeli, 2018). This process includes determining independent and dependent variables, controlling confounding factors, determining data collection methods, and designing experimental protocols to ensure the validity and reliability of the results (Fekra et al., 2021; Fard et al., 2021).

Box-Behnken Design (BBD) is an efficient method for experimental design that fits quadratic models with a minimum number of experiments by combining factors at intermediate levels. This method is especially useful when conducting extreme experiments (such as very high or low temperatures or pressures) is impractical or risky (Nam et al., 2018; Dbik et al., 2022). BBD is usually used for three or four factors and, with non-random combinations, provides suitable data for multinomial regression analysis. The main advantages of BBD are the reduction of cost and time of experiments compared to other methods such as central composite design (CCD) (Kashi et al., 2017; Bhattacharya, 2021). However, this method does not cover the entire factorial space and for very complex systems, supplementary methods may be required. In general, BBD is widely used in the food, chemical and pharmaceutical industries for process optimization (Latif et al., 2022).

It is clear that vitamin C, as a very important and widely used vitamin, is of great interest in the cosmetic, health and food industries. Extensive research has been conducted in this regard, but so far, magnetic nanoliposomization of these compounds has been studied less. The innovation of this research is the use of magnetic nanoliposomes as a carrier of vitamin C, which has not been reported so far.

2. Materials and methods

Chemicals

Phosphatidylcholine ($C_{42}H_{80}NO_8P \geq 99\%$), cholesterol ($C_{27}H_{46}O \geq 99\%$), chloroform ($CHCl_3 \geq 99\%$), citric acid ($C_6H_8O_7 \geq 99\%$), sodium hydroxide ($NaOH \geq 99\%$) were obtained from Sigma-Aldrich.

Methods

Synthesis of $CoFe_2O_4$ nanoparticles

To synthesize $CoFe_2O_4$ nanoparticles by sol-gel method, first dissolve the precursors cobalt nitrate and iron nitrate in a molar ratio of 1:2 in deionized water. Then, citric acid was added as a chelating agent and the solution was stirred until uniform. In the next step, the solution was adjusted to about $7-8$ by adding NaOH. Then, the mixture was slowly heated at 50 °C for 4 hours. Finally, the precipitate was dried at 80 °C after being centrifuged multiple times.

Synthesis of magnetic liposome/$CoFe_2O_4$ nanocarrier

First, 0.7 g of phosphatidylcholine and 0.3 g of cholesterol were dissolved in chloroform solvent at 45 °C and 150 rpm, and then a dry thin film was prepared under vacuum conditions in a rotary. In order to hydrate, sterile distilled water was added and left at 50 °C for 60 minutes. The next step involved adding $CoFe_2O_4$ nanoparticles in varying weight percentages to the synthesized nanoliposome. To reduce their size, they were then submerged in a bath sonicator set to 100 W Hz for 60 minutes.

Synthesis of magnetic liposome/$CoFe_2O_4$ encapsulated with ascorbic acid

First, 0.7 g of phosphatidylcholine and 0.3 g of cholesterol were dissolved in chloroform solvent at 45 °C with 150 rpm, and then a dry thin film was prepared under vacuum conditions in a rotary. Additionally, sterile distilled water was added and left at 50 °C for 60 minutes to hydrate the subject. Subsequently, ascorbic acid in varying concentrations and $CoFe_2O_4$ nanoparticles with varying weight percentages were added to the produced nanoliposome. Following that, they were submerged in a bath sonicator set to 100 W Hz of ultrasonic power for 60 minutes in order to shrink them.

Equipment used for characterization of nanoparticles

The XRD device examines the crystal structure of the material by irradiating the sample with X-rays and measuring the scattered rays. X-rays produced by the copper anode hit the sample and were diffracted according to Bragg's law. The detector recorded the angle and intensity of the diffracted rays and created a pattern of peaks, which can be analyzed to determine the lattice parameters, crystal phases, crystallite size and structural defects.

To investigate the functional groups of the synthesized nanoparticles, they were examined using a Brucker FTIR spectrometer. For this purpose, the samples were mixed and compressed with potassium bromide salt (KBr). To examine the functional groups, measurements of the infrared spectrum were made in the $400-4000$ cm^{-1} wavelength range. The best method to ensure the shape and structure of the nanoparticles is microscopic observation. The morphology of the produced nano-liposomes in terms of size, shape, and homogeneity was examined in this work using scanning and transmission electron microscopy. The size distribution range of the synthesized nanoparticles and also the peak size of the particles were determined using the dynamic light scattering (DLS) technique. This method is a technique used to measure the size of dissolved particles, with a size in the range of micrometers to nanometers. Also, to determine the amount of surface charge or Zeta Potential, which indicates the charge that a particle acquires in a specific environment, a Zeta-Sizer device was used at a temperature of 25 °C. Zeta potential is a suitable parameter to display the magnetic attraction between particles. The Vibrating Sample Magnetometer (VSM) is a precision instrument for measuring the magnetic properties of materials that works on the basis of Faraday electromagnetic induction. In this method, the sample vibrated at a certain frequency in a uniform magnetic field and this movement caused an induced current in the coils around the sample. The intensity and direction of this current are proportional to the magnetic moment of the sample and by changing the applied field, a hysteresis curve (hysteresis loop) was drawn.

Thermogravimetric Analysis (TGA) is a method for studying the mass changes of a sample due to temperature changes in a controlled atmosphere (such as nitrogen or air). In this method, the sample is placed in a furnace and its mass is continuously recorded by a sensitive balance as the temperature is programmed to increase. The weight loss or gain of synthesized nanoparticles is due to processes such as evaporation, thermal decomposition, oxidation, or chemical reactions. Optimization of ascorbic acid absorption using Box-Behnken design (BBD) methodology.

The BBD method was used to optimize the ascorbic acid absorption. The effective parameters including initial ascorbic acid concentration ($10-50$ mg/L), pH ($5-9$), time ($10-30$ min), and weight percentage of $CoFe_2O_4$ nanoparticles ($10-20\%$) were investigated at three different levels. Using the experimental design software, different combinations of these parameters were created and the effect of each on the absorption efficiency was evaluated. The optimal conditions were predicted by the mathematical model derived from the experimental data, which also explained the relationship between the independent variables and the ascorbic acid absorption efficiency by liposome/$CoFe_2O_4$ nanocarrier. Table 1 demonstrations the experiments designed using the Box-Behnken method.

Study of drug release process

To study the drug release process from the drug nanocarrier in a laboratory environment, the dialysis bag method was used under physiological body conditions (temperature 37 °C and pH 7.4) for 24 hours. In this approach, 1 mL of liposomal formulation incorporating yarrow extract was introduced into the dialysis bag, which was subsequently agitated within a controlled environment containing PBS buffer. Subsequently, at predetermined intervals ranging from 1 to 24 hours, aliquots of PBS buffer were extracted from the vicinity of the bag, and their absorptive characteristics were quantified utilizing a spectrophotometer set

Table 1. Experiments designed using the BBD method.

STD	RUN	Ascorbic acid (mg/L)	pH	Time (min)	$CoFe_2O_4$ (wt%)	Absorption (%)
26	1	30	7	20	15	72.41
20	2	50	7	30	15	63.96
4	3	50	9	20	15	78.92
19	4	10	7	30	15	81.37
14	5	30	9	10	15	88.29
9	6	10	7	20	10	79.67
10	7	50	7	20	10	49.01
24	8	30	9	20	20	75.48
2	9	50	5	20	15	55.74
27	10	30	7	20	15	72.44
5	11	30	7	10	10	66.92
12	12	50	7	20	20	60.22
8	13	30	7	30	20	70.69
7	14	30	7	10	20	60.11
22	15	30	9	20	10	91.38
17	16	10	7	10	15	83.22
16	17	30	9	30	15	98.42
21	18	30	5	20	10	57.13
3	19	10	9	20	15	99.99
1	20	10	5	20	15	79.32
6	21	30	7	30	10	64.76
13	22	30	5	10	15	62.65
11	23	10	7	20	20	60.54
29	24	30	7	20	15	72.16
28	25	30	7	20	15	72.86
23	26	30	5	20	20	57.08
18	27	50	7	10	15	54.38
15	28	30	5	30	15	62.85
25	29	30	7	20	15	72.22

to a peak wavelength of 267 nm. It is important to highlight that for each procedural phase, an identical volume of buffer was utilized, and a fresh buffer maintained at the same temperature was substituted. Subsequently, 1 mL of the suspension was extracted, subjected to filtration, and subsequently injected into the high-performance liquid chromatography (HPLC) apparatus. The device was replenished with 1 mL of PBS immediately following the removal of the suspension. All experimental trials were conducted in triplicate.

Study of *ex-vivo* permeability

An *ex-vivo* permeability investigation was conducted on optimized magnetic nanoliposomes containing free ascorbic acid solution in ethanol (serving as the control solution) across human dermal tissue utilizing Franz diffusion cells with a vertical orientation and an operational diffusion area of 1.4 cm^2. Human dermal specimens were procured from abdominoplasty procedures and preserved at −20 °C for no less than 24 hours (Samadi et al., 2020). The resected skin was rinsed with isotonic saline and positioned between the donor and recipient compartments of Franz diffusion cells, ensuring that the epidermal surface of the donor compartment faced inward. The recipient compartment was filled with 15 mL of PBS solution (pH 7.4), which was subjected to continuous agitation via a small magnetic stirrer at a controlled temperature of 37 ± 2 °C throughout the experimental protocol. A volume of 1 mL from each nanoliposome, magnetic nanoliposome, and a control sample containing an equivalent concentration of ascorbic acid (11 mg/L) was systematically administered onto the skin surface within the donor chamber. At predetermined intervals (1, 2, 3, 4, 5, 6, 7, 8, 10, 12, 16, 20, and 24 hours), the obtained solution was subjected to analysis for ascorbic acid concentration via HPLC. All experiments were conducted in triplicate. Human skin samples from abdominoplasty were prepared by

Stem Cell Technology Company with ethical approval from the Research Ethics Committee of the University of Tehran (No. [IR.IAU.CTB.REC.1404.026]) and in accordance with the Declaration of Helsinki. Informed consent was obtained from donors with full information about the aims, methods, risks, and right to withdraw.

3. Results and discussion

Characterization

X-ray diffraction (XRD) is an important analytical method for investigating the crystal structure and morphology of liposome nanoparticles. Liposomes, due to the amorphous or semi-crystalline structure of phospholipids, usually show broad and low-intensity diffraction patterns in XRD, indicating short-range order in the lipid bilayers.

Fig. 1 shows the XRD pattern for liposome and liposome/$CoFe_2O_4$ nanocarrier. Based on the results, the liposome nanoparticles are amorphous. The amorphous properties of liposomes, as derived from their XRD pattern, allow for their easy hydration. In the XRD spectrum for liposome/$CoFe_2O_4$ nanocarrier, the (111), (022), (113) and (222) planes at 2θ angles of 19.38°, 30.25°, 35.63° and 37.27° correspond to the standard card 96-591-0064, which is related to $CoFe_2O_4$ nanoparticles. This confirms the successful integration of crystalline $CoFe_2O_4$ within the amorphous liposome matrix, preserving the magnetic properties of the nanoparticles while leveraging the biocompatibility and flexibility of the liposomes.

The FTIR spectra were analyzed to determine the chemical interactions between the components of the liposome, liposome/$CoFe_2O_4$, and liposome/$CoFe_2O_4$/ascorbic acid as well as the functional groups. As shown in Fig. 2, the spectrum of liposome nanoparticles showed distinct bonds in the range of $1080 - 3400$ cm^{-1}, which can be attributed to the stretching and bending vibration of hydroxyl bonds (band at 3400 cm^{-1}), the asymmetric and symmetric stretching of -CH_3 (2923 cm^{-1}), and the asymmetric and symmetric stretching vibration of -CH_2 group (2853.5 cm^{-1}). The bond in the range of 1636 cm^{-1} is attributed to the stretching of ester group in lipids. In $CoFe_2O_4$ nanoparticles, the absorption feature observed at 602 cm^{-1} substantiates the existence of metal-oxygen interactions within the structural framework of $CoFe_2O_4$ magnetic nanoparticles. Additionally, it can be asserted that the mean absorption detected at 3405 cm^{-1} pertains to $CoFe_2O_4$ magnetic nanoparticles, which exhibits a spectral overlap with liposome nanoparticles. In the FTIR spectrum of ascorbic acid, there are distinct bonds in the region of 3400 cm^{-1} due to the O-H stretching of hydroxyl groups, in the region of 1638 cm^{-1} related to the C=O stretching of the carboxylic acid group, and in the region of 1383 cm^{-1} related to the C-O stretching (Fig. 2). In particular, key functional groups of ascorbic acid, such as O-H (ca. $3200 - 3400$ cm^{-1}), C=O (ca. $1650 - 1750$ cm^{-1}) and C-O-C (ca. $1000 - 1200$ cm^{-1}), showed intensity changes due to hydrogen bonding or electrostatic interactions with the liposome phospholipid headgroups (PO_4^{3-} at ca. 1230 cm^{-1} or C=O at ca. 1730 cm^{-1}) and the $CoFe_2O_4$ surface (Fe-O bonds at ca. $400 - 600$ cm^{-1}).

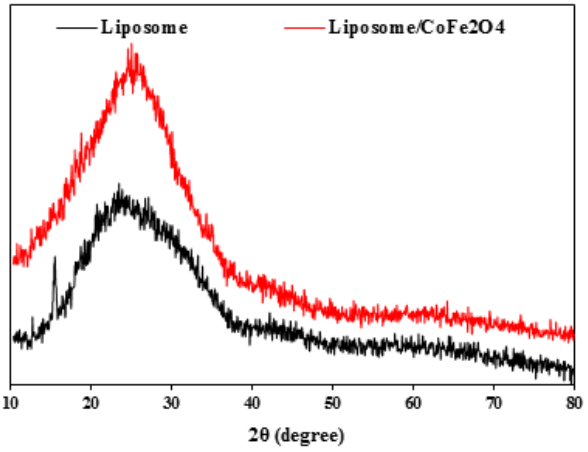

Figure 1. XRD for liposome and liposome/$CoFe_2O_4$ nanoparticles.

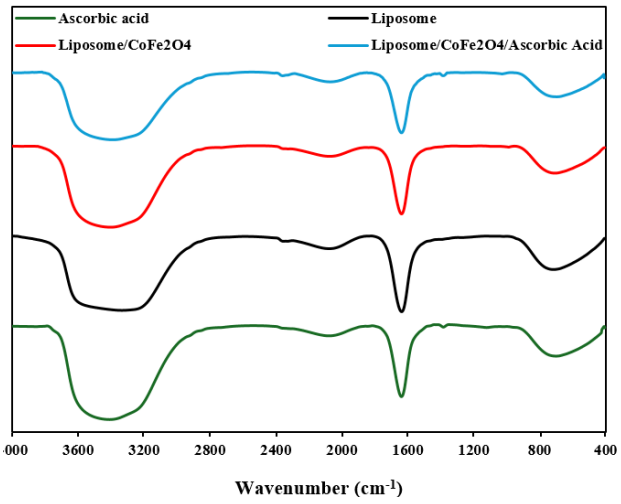

Figure 2. FTIR for ascorbic acid, liposome, liposome/$CoFe_2O_4$, and liposome/$CoFe_2O_4$/ascorbic acid.

Scanning Electron Microscopy (SEM) images of pure liposomes show uniform spherical structures with smooth surfaces and nanometer-sized vesicles ($50 - 150$ nm), which are typical features of liposomal vesicles. In contrast, SEM images of the liposome/$CoFe_2O_4$/ascorbic acid nanocarrier reveal clear changes in the surface morphology, such that $CoFe_2O_4$ nanoparticles are observed as bright and scattered spots on the surface of the liposomes, leading to surface roughness and an increase in the overall particle size ($150 - 200$ nm). These observations confirm that the magnetic nanoparticles have been successfully loaded onto the liposomes and the hybrid structure has been formed, while the overall uniformity and integrity of the liposomes have been maintained (Fig. 3 (a) and (b)).

Transmission electron microscopy (TEM) images of pure liposomes show uniform spherical structures with well-defined bilayer walls, confirming the classical features of liposomal vesicles. In contrast, TEM images of the liposome/$CoFe_2O_4$ nanocarrier revealed the presence of $CoFe_2O_4$ nanoparticles inside the liposome cavity or attached to its external surface, which was accompanied by local darkening and higher contrast in the image. These

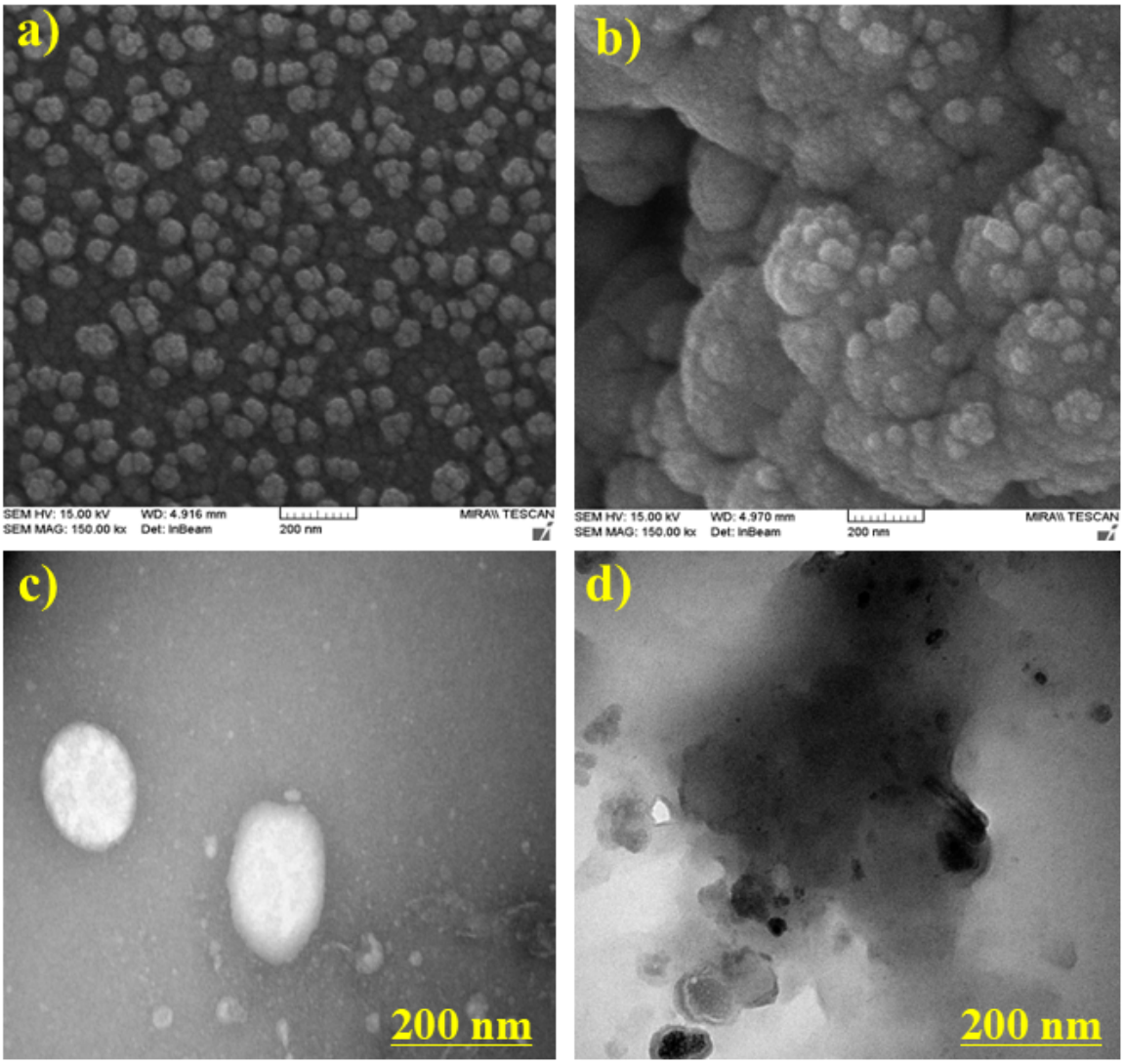

Figure 3. SEM for (a) liposome, (b) liposome/$CoFe_2O_4$/ascorbic acid, and TEM for (c) liposome, (d) liposome/$CoFe_2O_4$/ascorbic acid.

observations not only confirmed the success of nanoparticle loading, but also indicated that the liposome structure was maintained after loading. The uniform distribution of nanoparticles in the TEM images demonstrated the efficiency of the synthesis method in forming a unified nanocomposite (Fig. 3 (c) and (d)).

The energy dispersive X-ray spectroscopy (EDS) of the liposome/$CoFe_2O_4$ mainly confirmed the presence of the main constituent elements of the liposome, such as carbon (C), oxygen (O), and phosphorus (P), which are related to the phospholipid structure and organic compounds of the liposome. In addition to these elements, the presence of distinct peaks of cobalt (Co) and iron (Fe) was also revealed, which is a proof of the successful loading of $CoFe_2O_4$ nanoparticles on the liposome. The ratio of metal elements identified in this analysis can be used to quantitatively assess the loading of nanoparticles (Fig. 4).

As mentioned, the size of the synthesized nanocarrier was determined by DLS. The results of DLS (Fig. 5) presented that the size of the synthesized liposome and liposome/$CoFe_2O_4$ nanocarriers was 139 and 174 nm, respectively. Also, their dispersion index was determined to be 0.364 and 0.421, respectively. The experiments were repeated three times at this stage.

The zeta potential of the synthesized liposome and liposome/$CoFe_2O_4$/ascorbic acid nanocarrier nanocarriers was measured with a zeta sizer. The results of this device showed that the average surface charge of the synthesized liposome and liposome/$CoFe_2O_4$/ascorbic acid nanocarrier was -27.3 and -4.6 mV, which indicates that the resulting nanocarrier is of the anionic type that has less toxicity.

TGA results for liposome and liposome/$CoFe_2O_4$ nanocarrier are shown in Fig. 6. For liposomes in the temperature range of 100 °C, the weight loss is mainly due to the evaporation of absorbed water and moisture in the liposome structure and the decomposition of organic components of the liposome. For the liposome/$CoFe_2O_4$ nanocomposite, it indicates several stages of thermal degradation. In the temperature range of $25-130$ °C, the weight loss is mainly due to the evaporation of absorbed water and moisture in the liposome structure. At temperatures of $130-500$ °C, the decomposition of the organic components of the liposome (such as phospholipids and cholesterol) occurs, leading to a significant weight loss. At higher tempera-

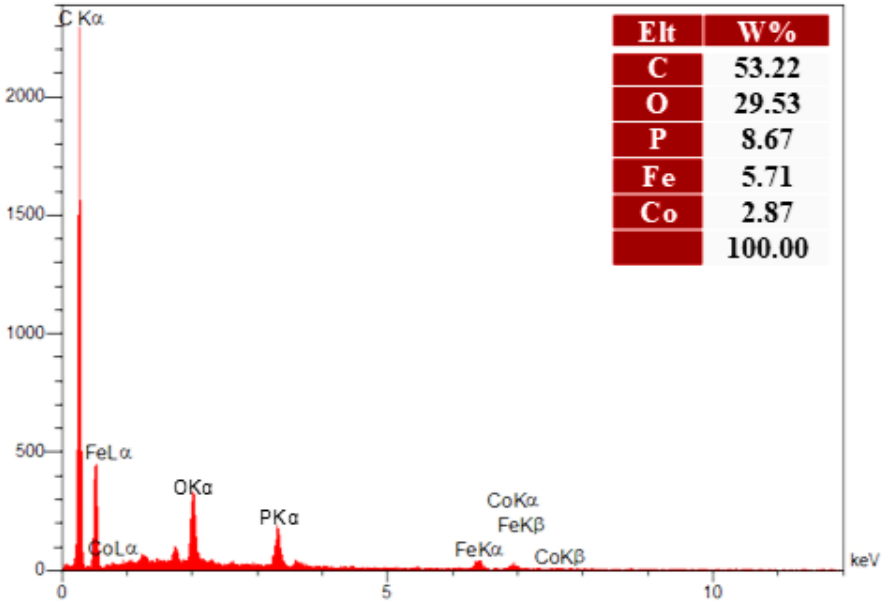

Figure 4. EDS results for liposome/$CoFe_2O_4$.

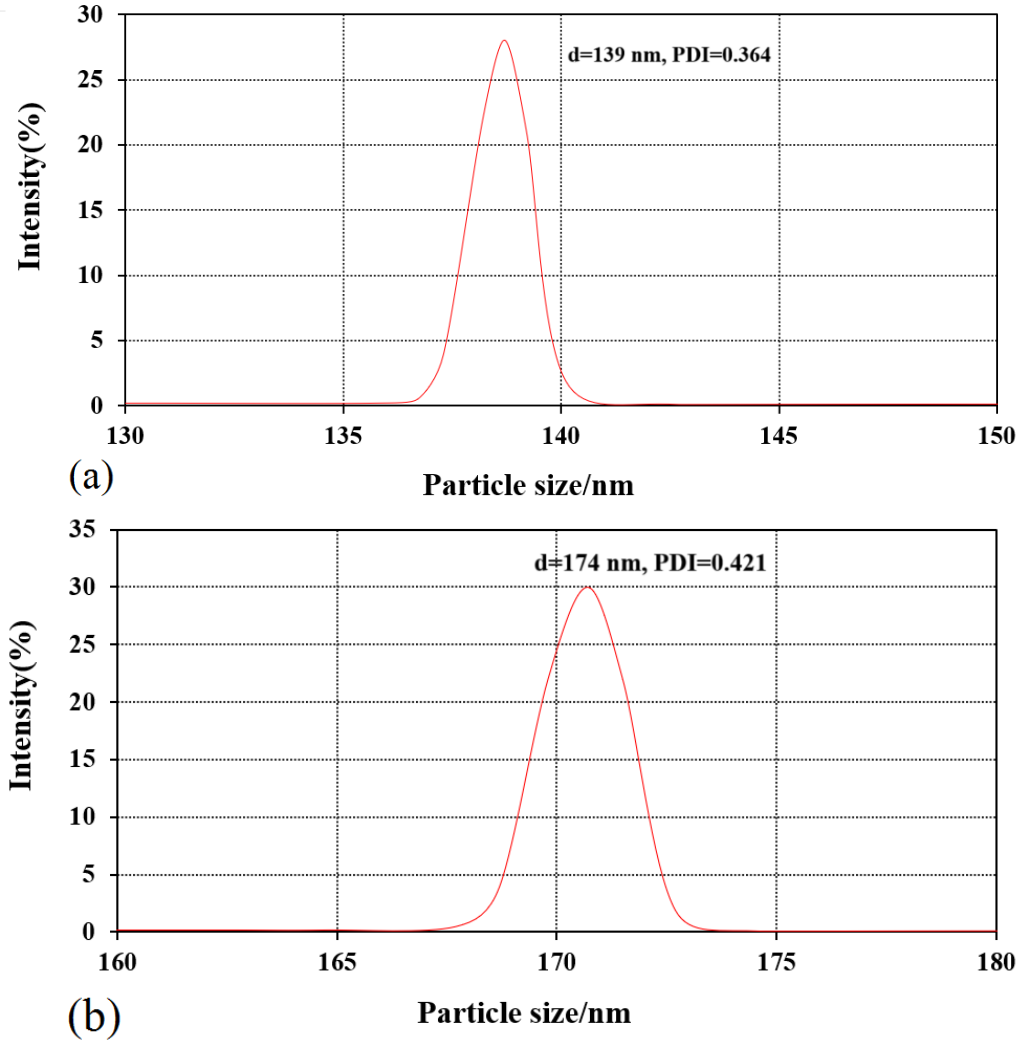

Figure 5. Diagram and table of the size of synthesized (a) liposome and (b) liposome/$CoFe_2O_4$/ascorbic acid nanocarrier in nanometers using the nano sizer device.

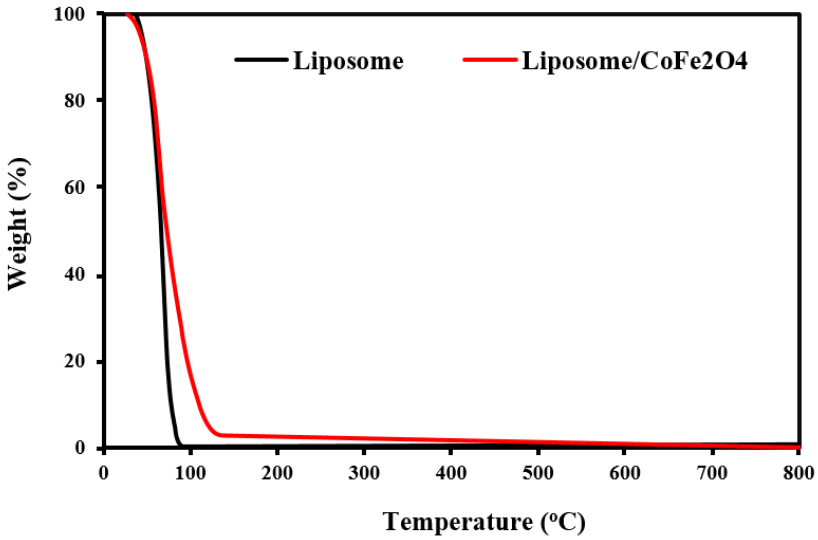

Figure 6. TGA results for liposome and liposome/$CoFe_2O_4$ nanocarrier.

tures ($500-800$ °C), the carbonaceous residues resulting from liposome degradation are oxidized and the $CoFe_2O_4$ nanoparticles remain as the stable inorganic phase. This analysis confirms that the liposome is well loaded on the nanoparticles and the nanocomposite has acceptable thermal stability.

For $CoFe_2O_4$ nanoparticles, it shows a hard ferromagnetic behavior with a relatively high coercivity (Hc) and a significant magnetic saturation (Ms). The M-H curve shows a clear hysteresis at room temperature, indicating magnetic stability and the ability to retain magnetization after removal of the external field. The Ms value obtained for $CoFe_2O_4$ is 63.27 emu/g. For the liposome/$CoFe_2O_4$ nanocomposite, it shows a soft ferromagnetic behavior with a magnetic saturation of 14.28 emu/g (Fig. 7). These characteristics indicate that the $CoFe_2O_4$ nanoparticles retain their magnetic properties even after loading on the liposome.

Experimental design

Analysis of Variance (ANOVA) was used to evaluate the statistical significance of the regression model and the effect of each of the independent parameters (ascorbic acid concentration, time, weight percent $CoFe_2O_4$ and pH) on the absorption response. The ANOVA results showed that the regression model was significant with a p-value less than 0.05 (usually < 0.001) at the 95% confidence level, indicating the suitability of the model for predicting the absorption efficiency. Also, the high F-values for the model and individual parameters indicated a strong effect of these variables on the absorption process. The coefficient of determination (R^2) above 0.85 also confirmed that the model was able to explain more than 90% of the response variations, indicating a good fit of the model with the experimental data (Table 2).

The normality of the data was examined using the nor-

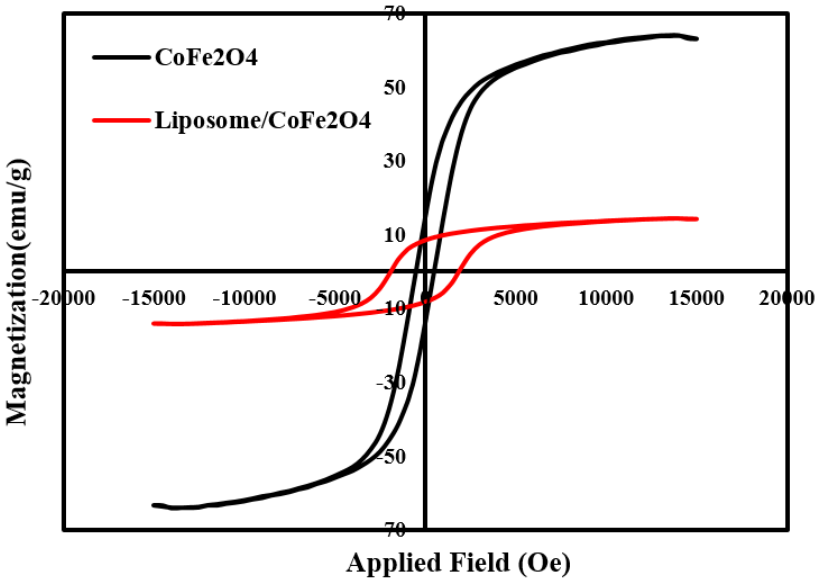

Figure 7. VSM results for liposome and liposome/$CoFe_2O_4$ nanocarrier.

Table 2. The BBD for the 4 independent variables.

Source	Sum of squares	Degree of freedom	Mean square	F-value	P-value Prob > F	
Model	4646.10	14	331.86	39.26	< 0.0001	significant
A-Ascorbic acid concentration	1237.89	1	1237.89	146.44	< 0.0001	
B-pH	2072.70	1	2072.70	245.20	< 0.0001	
C-Time	58.43	1	58.43	6.91	0.0198	
D-$CoFe_2O_4$	51.05	1	51.05	6.04	0.0276	
AB	1.58	1	1.58	0.1863	0.6726	
AC	32.66	1	32.66	3.86	0.0695	
AD	230.13	1	230.13	27.22	0.0001	
BC	24.65	1	24.65	2.92	0.1098	
BD	62.81	1	62.81	7.43	0.0164	
CD	40.58	1	40.58	4.80	0.0459	
A^2	11.60	1	11.60	1.37	0.2610	
B^2	255.52	1	255.52	30.23	< 0.0001	
C^2	0.0343	1	0.0343	0.0041	0.9501	
D^2	415.77	1	415.77	49.19	< 0.0001	
Residual	118.34	14	8.45			
Lack of Fit	118.04	10	11.80	156.51	< 0.0001	significant
Pure Error	0.3017	4	0.0754			
Cor Total	4764.44	28				

mal probability plot of residuals. The results showed that the points in the normal probability plot were linearly distributed and also confirmed the assumption of normality of the data with a p-value greater than 0.05 (0.12). These investigations confirm that the data used follow a normal distribution and therefore parametric analyses such as ANOVA and regression can be used to evaluate the model (Fig. 8 (a)). As can be seen in Fig. 8 (b), the pH parameter had the highest effect on the ascorbic acid absorption process. In the ascorbic acid absorption process by magnetic nanoliposomes containing $CoFe_2O_4$, the pH parameter has the highest effect, because pH affects both the surface charge of the nanoparticles and the ionic form of ascorbic acid.

Investigation and optimization of parameters

Four different parameters were evaluated to investigate the absorption of ascorbic acid by the nanocarrier. With increasing ascorbic acid concentration, the absorption efficiency decreases because the active absorption sites on the surface of $CoFe_2O_4$ nanoparticles/liposomes are no longer able to adsorb more molecules after reaching a saturated state. At low concentrations, the ratio of the number of ascorbic acid molecules to absorption sites is low and almost all molecules are adsorbed; however, with increasing concentration, the number of ascorbic acid molecules exceeds the absorption capacity of the nanoparticles, resulting in a decrease in the relative absorption percentage. Furthermore, at high concentrations, the probability of molecules competing for absorption to the active sites increases and some of them remain due to the kinetic and thermodynamic limitations of the absorption process. Also, the possible aggregation of ascorbic acid molecules in the solution can negatively affect their interaction with the surface of nanoparticles.

With increasing ascorbic acid concentration, the adsorption efficiency decreased because the active adsorption sites on the surface of $CoFe_2O_4$ nanoparticles/liposomes were no longer able to adsorb more molecules after reaching a saturated state. At low concentrations, the ratio of the number of ascorbic acid molecules to adsorption sites is low and therefore all molecules were adsorbed. However, with increasing concentration, the number of ascorbic acid molecules exceeded the adsorption capacity of the nanoparticles and, as a result, the relative adsorption percentage decreased. In addition, at high concentrations, the probability of molecules competing for adsorption to the active sites increased and some of them remained due to kinetic and thermodynamic limitations of the adsorption process. However, ascorbic acid molecules may aggregate in the solution, which could impair their ability to interact with the nanoparticle surface. The adsorption of ascorbic acid by liposomes/$CoFe_2O_4$ is most efficient at pH 8 due to the balance between the surface charge of the nanoparticles and the chemical form of ascorbic acid.

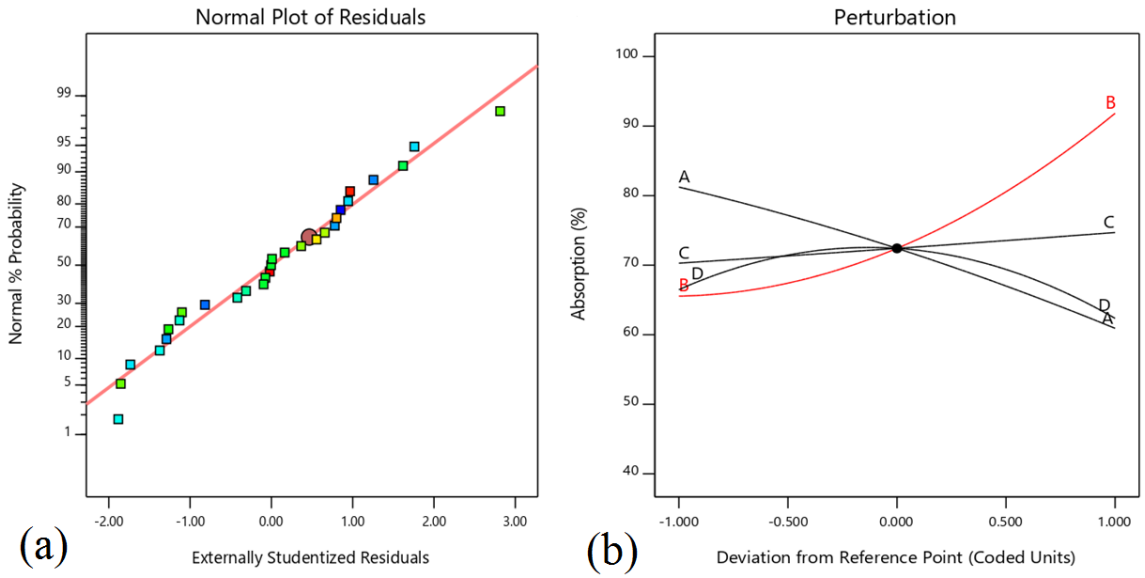

Figure 8. (a) normal plot of residuals and (b) perturbation plot.

Physiological skin conditions like sweat and sebum significantly affect the release and permeation of vitamin C from $CoFe_2O_4$ nanoparticles. Sweat (pH $4-6$) may enhance vitamin C dissolution but dilute its concentration, while sebum's lipid barrier can impede release and diffusion. Skin pH variations and sebum interactions may also destabilize vitamin C or alter nanoparticle properties, impacting bioavailability. In vitro studies with physiological mimics are essential to predict *in vivo* performance. To examine the impact of pH, experiments were carried out. In an alkaline environment (pH $= 8$), the hydroxyl groups of ascorbic acid are negatively charged and anionic, while the surface of the liposome/$CoFe_2O_4$ nanocarrier at this pH has a slight positive charge. Ascorbic acid and the liposome/$CoFe_2O_4$ nanocarrier are more strongly attracted to each other electrostatically as a result of this charge differential. Liposomes are also more stable at pH $= 8$ and their phospholipid membrane interacts better with ascorbic acid molecules. On the other hand, at acidic pH, ascorbic acid is in a neutral form and the electrostatic attraction is weaker (Fig. 9 (a)).

The effect of time on the adsorption of ascorbic acid by liposome/$CoFe_2O_4$ nanocarrier, the contact time between the nanocarrier and ascorbic acid plays a key role in the adsorption efficiency. Studies showed that in the early stages, the adsorption was rapid, which was due to the presence of abundant active sites on the surface of liposome/$CoFe_2O_4$ nanocarrier and the electrostatic interactions between it and ascorbic acid molecules. With increasing time, the adsorption rate remained almost constant after reaching equilibrium. This phenomenon occurs due to the saturation of the adsorption sites and the decrease of the driving force for further transport of molecules (Fig. 9 (b)).

Moreover, the best weight percentage of $CoFe_2O_4$ in liposomes for ascorbic acid adsorption was obtained at about 13%, because this value creates an optimal balance between increasing the adsorption sites and maintaining the stability of the liposomal structure. At values less than 13%, the number of cobalt ferrite nanoparticles is not sufficient to provide the desired active surface for ascorbic acid adsorption. On the other hand, at higher percentages (more than 15%), although the adsorption sites increase, the aggregation of nanoparticles increases and the stability of liposomes decreases, which leads to a decrease in the availability of active surfaces and a decrease in the adsorption efficiency. Also, high amounts of nanoparticles may disrupt the liposome structure and negatively affect its interaction with ascorbic acid. Therefore, 13% as the optimal point provides the greatest balance between the adsorption capacity and the stability of the system (Fig. 9 (c)).

Therefore, the optimal absorption time is usually a point that balances the initial absorption rate and the stability of the adsorbed complex. Under optimal conditions, the highest absorption rate was obtained with a concentration of ascorbic acid 11.99 mg/L, a time of 27.43 minutes, pH $= 8.78$ and a weight percentage of 13.85% $CoFe_2O_4$, equal to 99.99% (Fig. 10).

Study of *in vitro* release

The release kinetics of ascorbic acid from the optimized nanoliposome formulation and the pure ascorbic acid solution in PBS at pH 7.4 through the dialysis membrane were conducted over a 24-hour period (Fig. 11). The release profile of the control solution exhibited an initial burst release, with approximately half of the total drug (46%) being liberated within the first 4 hours. Subsequently, the release kinetics escalated to 86% from the 4-hour mark to the 12-hour interval, exhibiting an approximately linear trajectory from the 12-hour to the 24-hour period. In contrast, a consistent release of the drug devoid of any temporal delay was observed in the ascorbic acid nanoliposomes. As illustrated in Fig. 11, the quantity of drug released within the initial hour was below 20%, gradually achieving 86%

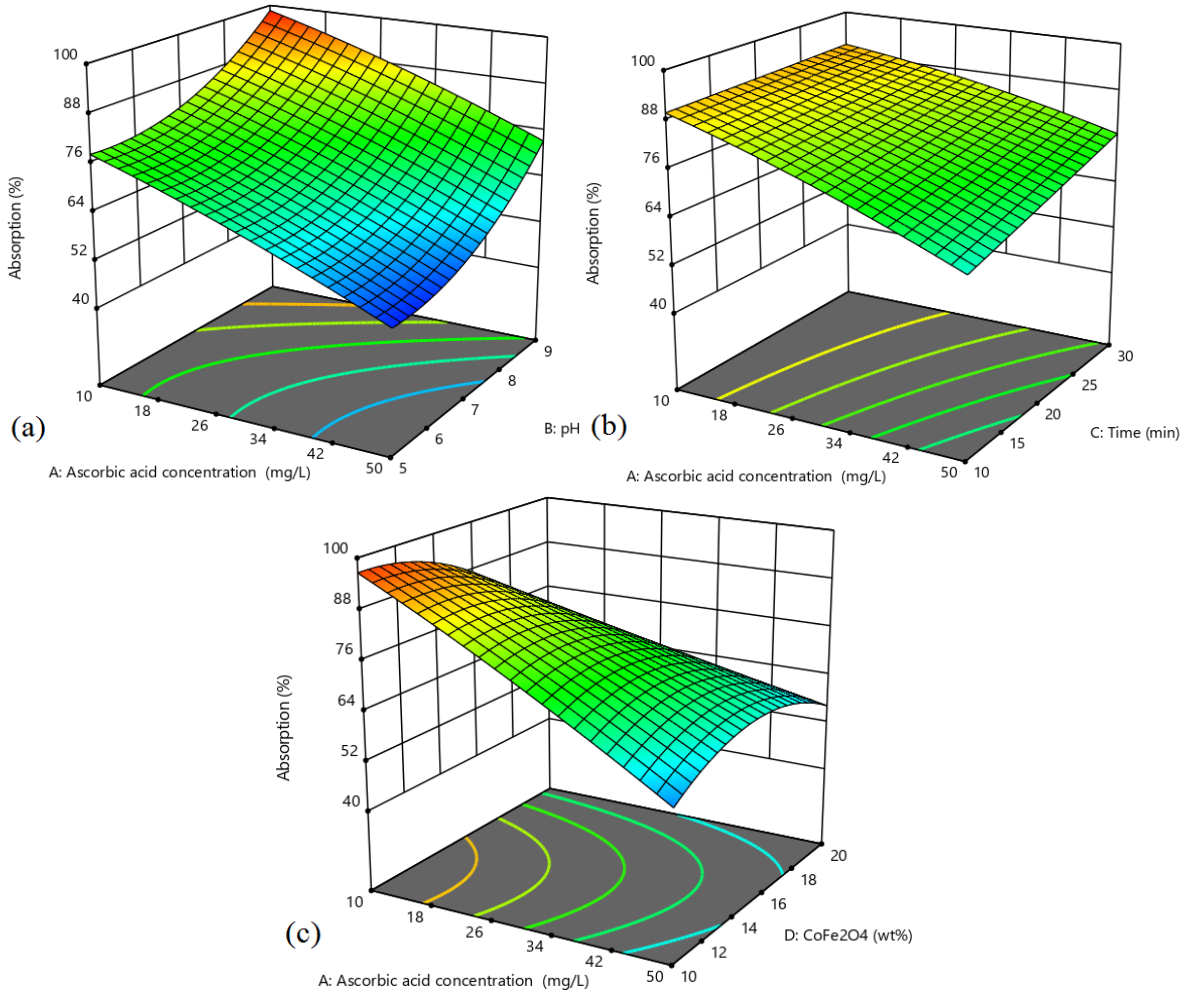

Figure 9. 3D diagram of the interaction of parameters (a) concentration of ascorbic acid and pH, (b) concentration of ascorbic acid and time, and (c) concentration of ascorbic acid and $CoFe_2O_4$ (wt%).

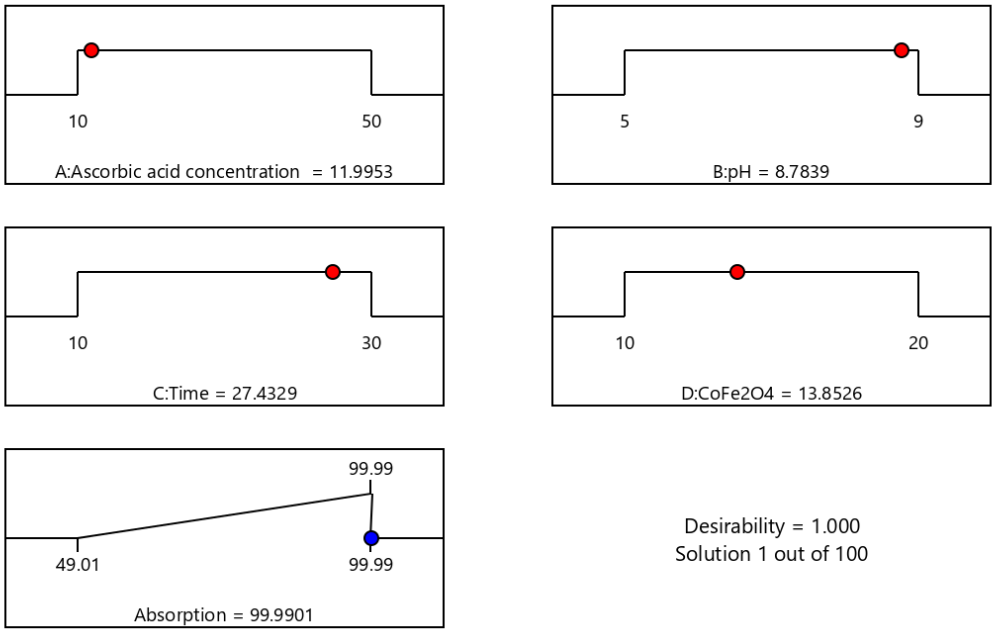

Figure 10. Optimization of ascorbic acid adsorption operating conditions.

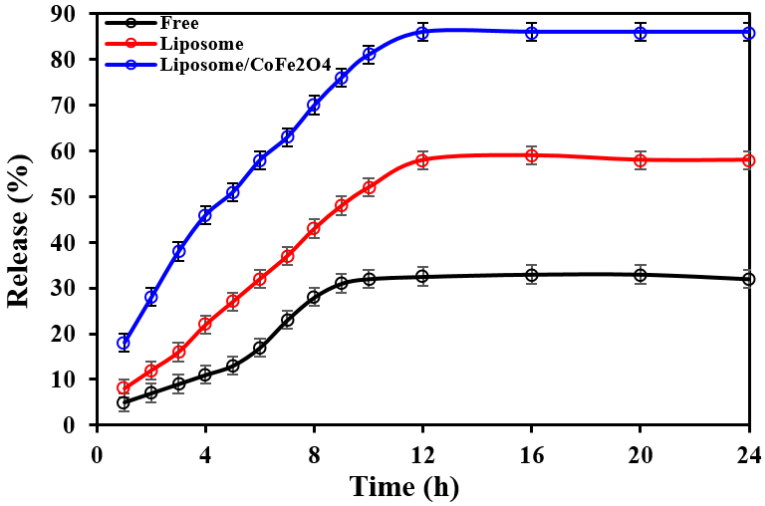

Figure 11. Drug release profiles *in vitro* for liposomes, free ethanolic solution, and optimized liposome/$CoFe_2O_4$/ascorbic acid.

by the 12-hour mark. Within nanoliposome formulations, the drug is required to traverse phospholipid and membrane barriers to access the receptor compartment, culminating in a sustained and regulated release profile when juxtaposed with a pure ascorbic acid solution.

Study of *ex-vivo* permeation

To assess the permeation characteristics of ascorbic acid-nanoliposomes, *ex-vivo* permeation investigations through human dermal tissue were conducted utilizing Franz vertical diffusion cells. The permeation metrics of the liposome/$CoFe_2O_4$ nanocarrier were juxtaposed with those derived from an equivalent concentration of the control formulation (ethanolic ascorbic acid solution, 11 mg/L). The permeation profiles of ascorbic acid (cumulative drug amount permeated against time) per unit area of skin from either the nanoliposomes or the control solution were quantified over a 24-hour period (Fig. 12). A notable surge in the permeation of ascorbic acid, with a total accumulation of under 60%, was recorded during the initial 8 hours, after which the rate of drug permeation remained relatively stable throughout all sampling intervals for the control solution. Conversely, no indications of an abrupt drug release from ascorbic acid-nanoliposomes were detected; thus, this characteristic of the nanoliposome formulation may contribute to a mitigation of sudden drug exposure to the dermal layer. Within the first eight hours, the ascorbic acid long-term penetration rate was reached. The ascorbic acid penetration rate then rose after 12 hours and leveled off. About 65 percent of the ascorbic acid encapsulated in nanoliposomes had directly penetrated the skin after 12 hours, with an amount of 623 μg/cm^2, whereas the amount of ascorbic acid that permeated from the control solution was only 226 μg/cm^2. We can conclude that the controlled release behavior and ascorbic acid encapsulation in nanoliposomes are critical elements for ascorbic acid's successful skin penetration. Ascorbic acid-nanoliposomes' efficient penetration is most likely due to the nanocarriers' tiny size. Studies on the skin penetration of vitamin C encapsulated in nanoliposomes produced reliable findings, demonstrating the significance of particle size in skin penetration.

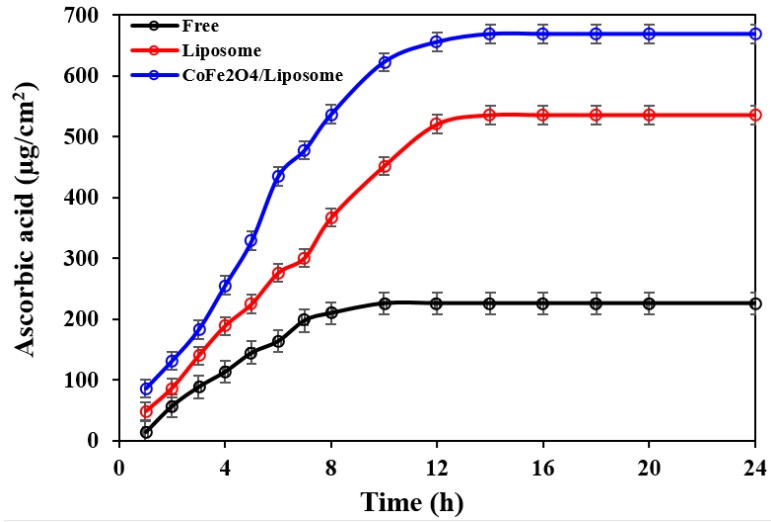

Figure 12. *Ex-vivo* permeation profile of free ascorbic acid, liposome, and liposome/$CoFe_2O_4$/ascorbic acid through human skin.

4. Conclusion

The study demonstrated the successful synthesis and characterization of a magnetic liposome/$CoFe_2O_4$/ascorbic acid nanocarrier for the encapsulation and controlled release of ascorbic acid. Under optimal conditions (11.99 mg/L ascorbic acid concentration, pH = 8.78, for 27.43 min, and 13.85 wt% $CoFe_2O_4$), the nanocarrier achieved a remarkable 99% absorption rate. Additionally, the release profile showed sustained delivery, with 84% of ascorbic acid released over 24 hours, contrasting sharply with the burst release observed in the pure ascorbic acid solution. The nanoliposome formulation ensured a gradual release, with less than 20% released in the first hour, reaching 86% by 12 hours, highlighting its potential for controlled drug delivery applications. *Ex-vivo* permeation studies using human skin revealed significant advantages of the ascorbic acid-nanoliposomes over the control solution. While the control exhibited a burst permeation of less than 60% in the first 8 hours, the nanoliposomes provided a steady, prolonged release without an initial burst, reducing sudden drug exposure to the skin. In conclusion, the magnetic liposome/$CoFe_2O_4$ nanocarrier offers a promising platform for the efficient encapsulation, sustained release, and enhanced skin permeation of ascorbic acid. The optimized formulation not only maximizes absorption but also ensures controlled delivery, minimizing burst release and improving long-term penetration. These findings underscore the potential of nanoliposome-based systems in dermatological and therapeutic applications, where controlled and effective drug delivery is critical. Further research could explore scalability and *in vivo* efficacy to validate these promising *ex-vivo* results. Additionally, potential scalability challenges, such as maintaining uniformity in nanoparticle synthesis and liposome stability during large-scale production, remain unaddressed. Future research should focus on *in vivo* efficacy studies, scalability assessments, and optimization of the experimental design to enhance model accuracy and ensure practical applicability of this promising nanocarrier system in therapeutic and dermatological contexts.

Authors contributions
Authors have contributed equally in preparing and writing the manuscript.

Availability of data and materials
The data that support the findings of this study are available from the corresponding author, upon reasonable request.

Conflict of interests
The authors declare that they have no known competing financial interests or personal relationships that could have appeared to influence the work reported in this paper.

References

Abdolmohammadi S., Shariati S., Fard N. E., Samani A. (2020) Aqueous-mediated green synthesis of novel spiro [indole-quinazoline] derivatives using kit-6 mesoporous silica coated Fe_3O_4 nanoparticles as catalyst. *J. Heterocycl. Chem.* 57 (7): 2729–2737. DOI: https://doi.org/10.1002/JHET.3981.

Ahmed K. S., Hussein S. A., Ali A. H., Korma S. A., Lipeng Q., Jinghua C. (2019) Liposome: composition, characterisation, preparation, and recent innovation in clinical applications. *J. Drug Target.* 27 (7): 742–761. DOI: https://doi.org/10.1080/1061186X.2018.1527337.

Akbari J., Saeedi M., Ahmadi F., Hashemi S. M. H., Babaei A., Yaddollahi S., Rostamkalaei S. S., Asare-Addo K., Nokhodchi A. (2022) Solid lipid nanoparticles and nanostructured lipid carriers: a review of the methods of manufacture and routes of administration. *Pharm. Dev. Technol.* 27 (5): 525–544. DOI: https://doi.org/10.1080/10837450.2022.2084554.

Alkilani A. Z., Nasereddin J., Hamed R., Nimrawi S., Hussein G., Abo-Zour H., Donnelly R. F. (2022) Beneath the skin: A review of current trends and future prospects of transdermal drug delivery systems.

Baek J., Ramasamy M., Willis N. C., Kim D. S., Anderson W. A., Tam K. C. (2021) Encapsulation and controlled release of vitamin C in modified cellulose nanocrystal/chitosan nanocapsules. *Curr. Res. Food Sci.* 4:215–223. DOI: https://doi.org/10.1016/j.crfs.2021.03.010.

Bhattacharya S. (2021) Central composite design for response surface methodology and its application in pharmacy. *Response Surface Methodology in Engineering Science. IntechOpen,* DOI: https://doi.org/10.5772/intechopen.95835.

Dbik A., El Messaoudi N., Bentahar S., El Khomri M., Lacherai A., Faska N. (2022) Optimization of methylene blue adsorption on agricultural solid waste using Box–Behnken design (BBD) combined with response surface methodology (RSM) modeling. *Biointerface Res. Appl. Chem.* 12 (4): 4567–4583. DOI: https://doi.org/10.33263/BRIAC124.45674583.

De Oliveira T. C., Tavares M. E., Soares-Sobrinho J. L., Chaves L. L. (2022) he role of nanocarriers for transdermal application targeted to lymphatic drug delivery: opportunities and challenges. *J. Drug Deliv. Sci. Technol.* 68:103110. DOI: https://doi.org/10.1016/j.jddst.2022.103110.

Elmi Fard N., Fazaeli R. (2022) Fabrication of superhydrophobic $CoFe_2O_4$/polyaniline/covalent organic frameworks/cotton fabric membrane and evaluation of its efficiency in separation of olive oil from water. *J. Chin. Chem. Soc.* 69 (12): 2014–2026. DOI: https://doi.org/10.1002/jccs.202200368.

Fard N. E., Fazaeli R. (2018) Optimization of operating parameters in photocatalytic activity of visible light active Ag/TiO_2 nanoparticles. *Russ. J. Phys. Chem. A* 92 (13): 2835–2846. DOI: https://doi.org/10.1134/S0036024418130071.

Fard N. E., Fazaeli R., Yousefi M., Abdolmohammadi S. (2021) Oxidative desulfurization of dibenzothiophene using M/TiO_2/MWW (M = Cu, Ag, and Au) composite. *Russ. J. Phys. Chem. A.* 95:S23–S32. DOI: https://doi.org/10.1134/S0036024421140065.

Fekra S. S., Fard N. E., Fazaeli R. (2021) Photocatalytic degradation of antibiotic norfloxacin aqueous solution by Ce/Bi_2WO_6: optimization and simulation of process by RSM. *Russ. J. Appl. Chem* 94 (6): 824–834. DOI: https://doi.org/10.1134/S1070427221060161.

Gupta V., Trivedi P. (2018) *In vitro* and *in vivo* characterization of pharmaceutical topical nanocarriers containing anticancer drugs for skin cancer treatment. *Lipid Nanocarriers for Drug Targeting,* 563–627. DOI: https://doi.org/10.1016/B978-0-12-813687-4.00015-3.

Jeong W. Y., Kwon M., Choi H. E., Kim K. S. (2021) Recent advances in transdermal drug delivery systems: a review. 25

Kashi N., Elmi Fard N., Fazaeli R. (2017) Empirical modeling and CCD-based RSM optimization of Cd(II) adsorption from aqueous solution on clinoptilolite and bentonite. *Russ. J. Appl. Chem.* 90 (6): 977–992. DOI: https://doi.org/10.1134/S1070427217060210.

Latif A., Maqbool A., Zhou R., Arsalan M., Sun K., Si Y. (2022) Optimized degradation of bisphenol A by immobilized laccase from Trametes versicolor using Box–Behnken design (BBD) and artificial neural network (ANN). *J. Environ. Chem. Eng.* 10 (2): 107331. DOI: https://doi.org/10.1016/j.jece.2022.107331.

Nam S.-N., Cho H., Han J., Her N., Yoon J. (2018) Photocatalytic degradation of acesulfame K: optimization using the Box–Behnken design (BBD). *Process Saf. Environ. Prot.* 113:10–21. DOI: https://doi.org/10.1016/j.psep.2017.09.002.

Pisoschi A. M., Pop A., Cimpeanu C., Turcuş V., Predoi G., Iordache F. (2018) Nanoencapsulation techniques for compounds and products with antioxidant and antimicrobial activity – a critical view. *Eur. J. Med. Chem.* 157:1326–1345. DOI: https://doi.org/10.1016/j.ejmech.2018.08.076.

Queiroz J. L. C. de, Medeiros I., Trajano A. C., Piuvezam G., Franca Nunes A. C. de, Passos T. S., Araujo Morais A. H. de (2022) Encapsulation techniques perfect the antioxidant action of carotenoids: a systematic review of how this effect is promoted. *Food Chem.* 385:132593. DOI: https://doi.org/10.1016/j.foodchem.2022.132593.

Samadi N., Azar P. A., Husain S. W., Maibach H. I., Nafisi S. (2020) Experimental design in formulation optimization of vitamin K1 oxide-loaded nanoliposomes for skin delivery. *Int. J. Pharm* 579:119136. DOI: https://doi.org/10.1016/j.ijpharm.2020.119136.

Sun Q., Yin S., He Y., Cao Y., Jiang C. (2023) Biomaterials and encapsulation techniques for probiotics: current status and future prospects in biomedical applications. *Nanomater* 13 (15): 2185. DOI: https://doi.org/10.3390/nano13152185.

Vandani S. A. K., Kalaee M., Saravani M. G., Fard N. E., Rahmati M., Kamani M. (2023) Preparation of magnetic Fe_3O_4/MoO_3/MCM-22 photocatalyst and its study on metronidazole adsorption, degradation, and process optimization. *Russ. J. Phys. Chem. A* 97 (4): 618–632. DOI: https://doi.org/10.1134/S003602442304026X.

Wang S., Chen Y., Guo J., Huang Q. (2023) Liposomes for tumor targeted therapy: a review. *Int. J. Mol. Sci.* 24 (3): 2643. DOI: https://doi.org/10.3390/ijms24032643.

Xiao Y., Tan A., Jackson A. W., Boyd B. J. (2022) Nonspherical nanocapsules as long-circulating drug delivery systems. *Chem. Mater.* 34 (6): 2503–2530. DOI: https://doi.org/10.1021/acs.chemmater.1c03573.

Yin X., Chen K., Cheng H., Chen X., Feng S., Song Y., Liang L. (2022) Chemical stability of ascorbic acid integrated into commercial products: a review on bioactivity and delivery technology. *Antioxidants* 11 (1): 153. DOI: https://doi.org/10.3390/antiox11010153.